

# Silicate weathering and North Atlantic silica burial during the Paleocene-Eocene Thermal Maximum

Donald E. Penman

Geology & Geophysics, Yale University, New Haven, Connecticut 06520, USA

## ABSTRACT

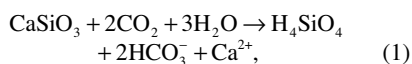
**During the Paleocene-Eocene Thermal Maximum (PETM, ca. 56 Ma), thousands of gigatons of carbon were released into the ocean and atmosphere over several thousand years, offering the opportunity to study the response of ocean biogeochemistry to a carbon cycle perturbation of a similar magnitude to projected anthropogenic CO<sub>2</sub> release. PETM scenarios typically invoke accelerated chemical weathering of terrestrial silicate rocks as a significant negative feedback driving the recovery and termination of the event. However, the implications of this mechanism for the geochemical cycling of silica during the PETM have received little attention. I use “back-of-the-envelope” calculations and a simple two-box geochemical model of the marine silica cycle to demonstrate that the sequestration of thousands of gigatons of carbon by enhanced silicate weathering during the PETM would have dramatically increased the riverine supply of dissolved silica (H<sub>4</sub>SiO<sub>4</sub>) to the oceans. This would have elevated seawater [H<sub>4</sub>SiO<sub>4</sub>], encouraging both increased opal (SiO<sub>2</sub>) production by siliceous organisms and enhanced preservation of SiO<sub>2</sub> in the water column and sediments. Both of these factors would have promoted a prompt (due to the relatively short oceanic residence time of silica) increase in sedimentary opal burial, thus balancing the marine silica budget. Several recently recovered deep-sea sedimentary records from the central North Atlantic demonstrate elevated SiO<sub>2</sub> content across the Paleocene-Eocene boundary, which I argue is the result of enhanced production and/or preservation of SiO<sub>2</sub> in response to elevated [H<sub>4</sub>SiO<sub>4</sub>] in the North Atlantic, representing the ultimate fate of excess Si weathered from the continents during the PETM.**

## INTRODUCTION

The Paleocene-Eocene Thermal Maximum (PETM) was the largest and most abrupt greenhouse warming event of the Cenozoic. Marine and terrestrial records document a global >3‰ negative carbon isotope excursion (CIE) (Kennett and Stott, 1991; McInerney and Wing, 2011) coincident with global surface warming of >4 °C (Dunkley-Jones et al., 2013) and geochemical and sedimentological evidence for ocean acidification (Penman et al., 2014; Zeebe and Zachos, 2007). These lines of evidence suggest a rapid (10<sup>3</sup>–10<sup>4</sup> yr) and massive (thousands of gigatons of carbon [GtC], similar to projected anthropogenic CO<sub>2</sub> emissions) release of <sup>13</sup>C-depleted carbon into the ocean-atmosphere system.

## WEATHERING FEEDBACKS DURING THE PETM

Elevated atmospheric *p*CO<sub>2</sub> and resulting surface warming and hydrologic cycle intensification are thought to accelerate the chemical weathering of terrestrial silicate rocks, commonly generalized (Berner et al., 1983) as:



in which CaSiO<sub>3</sub> (wollastonite) approximates the diversity of silicate minerals composing the

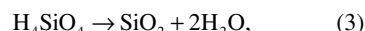
continents. Enhancing silicate weathering accelerates the delivery of dissolved inorganic carbon (DIC), alkalinity, and dissolved silica (H<sub>4</sub>SiO<sub>4</sub>) to the oceans. On long time scales (>10<sup>5</sup> yr), this alkalinity flux is balanced by carbonate production and burial:



The balance of silicate weathering (Equation 1) with carbonate burial (Equation 2) gives rise to a net consumption of CO<sub>2</sub> (buried as CaCO<sub>3</sub>). This CO<sub>2</sub> consumption in response to warming forms the basis of a long-term negative (stabilizing) feedback on climate, proposed to be important in maintaining habitable temperatures throughout Earth history (Berner et al., 1983) and specifically during the PETM (Kelly et al., 2010; Torfstein et al., 2010). Elevated silicate weathering during the PETM is supported by shifts in Os isotope records (Ravizza et al., 2001). Elevated carbonate burial following the initial acidification event is seen above the lysocline (Kelly et al., 2010), and as an “overshoot” of the carbonate compensation depth during the PETM recovery, with carbonates being preserved at deeper depths shortly after the event than before it (Penman et al., 2016).

However, enhanced weathering during the PETM should also have increased the riverine

supply of H<sub>4</sub>SiO<sub>4</sub> to the oceans, a consequence of this climate-stabilizing feedback that has not been fully explored. On long time scales, the riverine flux of H<sub>4</sub>SiO<sub>4</sub> (and minor dust and hydrothermal input) is balanced by precipitation and burial of biogenic opal (SiO<sub>2</sub>) (Racki and Cordey, 2000; Yool and Tyrrell, 2005; Fig. 1):



giving the net reaction for silicate weathering drawdown of CO<sub>2</sub> and burial of carbonate and opal (Equations 1 + 2 + 3):



In this contribution, I explore the magnitude of the Si-cycle perturbation during the PETM using “back-of-the-envelope” calculations and a geochemical model of the silica cycle, and present new sedimentary records from the North Atlantic that contain elevated SiO<sub>2</sub> across the PETM.

## HOW LARGE WAS THE Si CYCLE PERTURBATION DURING THE PETM?

Estimates for the mass of carbon released during the PETM based on the size of the CIE and the δ<sup>13</sup>C of possible sources (McInerney and Wing, 2011) extends from ~5000 GtC of

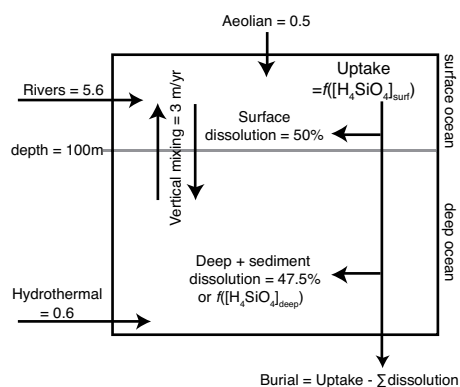


**Figure 1. Si-cycle model architecture showing fluxes in teramoles Si per year, after Racki and Cordey (2000), Treguer et al. (1995), and Yool and Tyrrell (2003). See the Data Repository (see footnote 1) for full model description and parameterizations (denoted *f*) in the figure of feedbacks.**

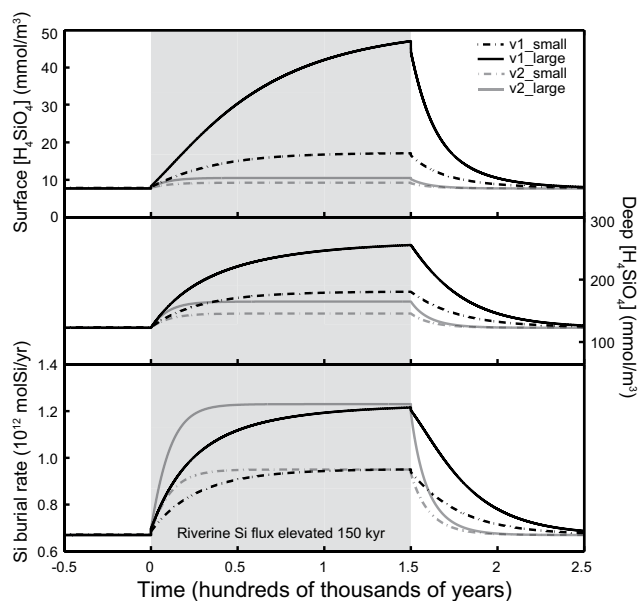
methane (e.g., Zeebe et al., 2009) to ~10,000 GtC of organic carbon (e.g., Cui et al., 2011). If all of that carbon were to be sequestered via the net silicate weathering feedback (Equation 4), this would release an extra  $4.2\text{--}8.3 \times 10^{17}$  mol of Si into the oceans. However, care must be taken with the assumption that wollastonite weathering (Equation 1), a simplification of the variety of silicate minerals and weathering pathways that occur at Earth's surface, is representative of the relevant fluxes of  $\text{CO}_2$  and Si—specifically the ratio of Si released relative to  $\text{CO}_2$  consumed. This ratio (1 mol Si : 2 mol  $\text{CO}_2$  in Equation 1) ranges in various weathering reactions from 0 to 3 (e.g., Garrels and Berner, 1983, and references therein). However, comparison of modern global  $\text{CO}_2$  consumption by silicate weathering ( $11.7 \times 10^{12}$  mol C/yr; Gaillardet et al., 1999) with the global riverine  $\text{H}_4\text{SiO}_4$  flux ( $5.6 \times 10^{12}$  mol Si/yr; Yool and Tyrrell, 2005) gives a global average of 0.48 mol Si released per mole  $\text{CO}_2$  consumed—very close to the 1:2 ratio in Equation 1. I therefore consider Equation 1 to describe globally averaged Si release during silicate weathering adequately for the present purpose.

The extra  $4.2\text{--}8.3 \times 10^{17}$  mol Si released by silicate weathering during the PETM would have been taken up by marine silicifying organisms and buried in sediments as 25,000–50,000 Gt  $\text{SiO}_2$ . This corresponds to a volume of 12,000–24,000  $\text{km}^3$  of opal, the equivalent of a thickness of 3.3–6.6 cm distributed over the entire seafloor. This is a significant volume of opal; however, as the PETM lasted ~150 k.y. (Murphy et al., 2010), the release of anomalous  $\text{H}_4\text{SiO}_4$  would have been distributed over a similar time interval, and its deposition as opal could conceivably have been even more protracted. Characterization of the Si-cycle perturbation during the PETM and the time scale of its response therefore requires consideration of the standing inventory and fluxes of Si into, out of, and within the ocean.

Toward that end, I employ a two-box geochemical model of the marine Si cycle (Fig. 1) based on the modern budget (Racki and Cordey, 2000; Treguer et al., 1995; Yool and Tyrrell, 2005). Several configurations of the model were run with various representations of Si-cycle feedbacks, with representative end-member results plotted in Fig. 2, and the full suite of model runs plotted and described in the GSA Data Repository<sup>1</sup>. The uptake of dissolved silica by siliceous plankton was described by various functions of surface  $[\text{H}_4\text{SiO}_4]$  meant to bracket the possible sensitivity of silicifiers to elevated riverine dissolved silica flux. The amount of opal export that survives dissolution in the water column

<sup>1</sup>GSA Data Repository item 2016239, plots of all model runs, Table DR1 (model architecture and constants), and description of the model runs as well as equations describing the feedbacks used, is available online at [www.geosociety.org/pubs/ft2016.htm](http://www.geosociety.org/pubs/ft2016.htm), or on request from [editing@geosociety.org](mailto:editing@geosociety.org).

**Figure 2. Modeled surface and deep  $[\text{H}_4\text{SiO}_4]$  and opal burial rate response to elevated riverine Si input. Solid and dashed lines represent maximum (10,000 gigatons carbon [GtC]) and minimum (5000 GtC) Paleocene-Eocene Thermal Maximum (PETM) forcings, respectively. Gray lines (model v2) use the most sensitive configuration of model, featuring linear response of global surface opal uptake to surface  $[\text{H}_4\text{SiO}_4]$  combined with opal burial fraction that responds to deep  $[\text{H}_4\text{SiO}_4]$ . Black lines (model v1) use a significantly less sensitive configuration, in which surface uptake asymptotes at double modern (to simulate other limitations on silicifiers, such as nutrients for diatoms and food supply for radiolarians; Yool and Tyrrell, 2003) and burial fraction is constant. See Data Repository (see footnote 1) for model description.**



and surface sediments to ultimately be buried was parameterized based on deep  $[\text{H}_4\text{SiO}_4]$ . To simulate the PETM Si-cycle perturbation, the model was forced with an increase in riverine  $\text{H}_4\text{SiO}_4$  input corresponding to the consumption by silicate weathering of the range of carbon release estimates (5000–10,000 GtC) from the above calculations distributed over the duration of the PETM (150 k.y.; Murphy et al., 2010). This gives an increase in riverine  $\text{H}_4\text{SiO}_4$  supply of 2.8–5.6 Tmol/yr during the event, representing as much as a doubling of riverine Si input.

Due to elevated Si supply, surface and deep  $[\text{H}_4\text{SiO}_4]$  begin to increase at the onset and approach new equilibria within the event (Fig. 2). In the most sensitive configurations of the model, surface  $[\text{H}_4\text{SiO}_4]$  increase is limited to only 7%–14% above pre-event levels (attained within 50 k.y. of the onset), whereas in configurations with weaker feedbacks, surface  $[\text{H}_4\text{SiO}_4]$  reaches levels up to five times higher and still rising by the end of the PETM. In all configurations of the model that incorporate any feedback at all on changing  $[\text{H}_4\text{SiO}_4]$ , opal burial rates respond to elevated input during the PETM (approaching or attaining a new steady state, wherein elevated riverine Si supply is balanced by elevated opal burial) and then relax over tens of thousands of years after the event. The cumulative excess opal burial by the end of the run is, due to mass balance requirements, equal to the prescribed total excess  $\text{H}_4\text{SiO}_4$  input, and in all cases at least 85% of this excess opal burial occurs before the end of the event (within 150 k.y.).

These estimates are subject to numerous sources of uncertainty, foremost the mass of carbon release, as well as boundary conditions which may have differed from modern due to the

reduced importance of diatoms over radiolarians (Harper and Knoll, 1975; Racki and Cordey, 2000) and a slightly higher background weathering rate during the warm late Paleocene (Muttoni and Kent, 2007). These differences could change the Si cycle's equilibration time scale (as noted by Yool and Tyrrell [2005]) but not the conclusion that elevated silicate weathering during the PETM requires elevated silica burial. The model focuses on pelagic production and burial of  $\text{SiO}_2$ , but it is possible that shelf sediments could have accommodated elevated  $\text{SiO}_2$  burial, as they did in response to Si-cycle perturbation through the Triassic-Jurassic boundary (Ritterbush et al., 2015), before the emergence of widespread pelagic silicifiers. Finally, it has been argued (Bowen and Zachos, 2010) that in addition to silicate weathering, the permanent burial of organic C (as much as 2000 GtC) aided the PETM recovery, which would make the calculation of silica input an overestimate. Taken at face value, a doubling of silicate weathering during the PETM would imply either a higher sensitivity of silicate weathering rates to  $p\text{CO}_2$  and/or temperature than has been assumed in carbon cycle simulations of the PETM (e.g. Dickens et al., 1997; Zeebe et al., 2009) or that those simulations underestimate the  $p\text{CO}_2$  and/or temperature rise during the PETM. Nevertheless, both simple calculations and modeling demonstrate that if estimates of carbon release during the PETM are at all accurate, and if a large fraction of this carbon was indeed sequestered by silicate weathering, then the Si cycle must have undergone a pronounced perturbation during the event. This would have resulted in elevated  $[\text{H}_4\text{SiO}_4]$  and the prompt burial of a large mass of  $\text{SiO}_2$  in sediments.

## NEW RECORDS OF SILICA BURIAL FROM THE NORTH ATLANTIC

Integrated Ocean Drilling Program (IODP) Expedition 342 penetrated the Paleocene-Eocene boundary on the Southeast Newfoundland Ridge (central North Atlantic) at Sites U1403 (39°56.60'N, 51°48.20'W), U1407 (41°25.5'N, 49°48.8'W), U1408 (41°26.3'N, 49°47.1'W), and U1409 (41°17.75'N, 49°14.00'W) (Fig. 3). Shipboard investigation described lithology using visual core description, smear slides, and weight percent CaCO<sub>3</sub>, and identified the position of the Paleocene-Eocene boundary at each site via biostratigraphy (Norris et al., 2012). Subsequent bulk carbonate and organic carbon δ<sup>13</sup>C records documented the PETM CIE at Sites U1403 and U1409 (Penman et al., 2016).

Site U1403 features a transition from upper Paleocene carbonate-barren clay to lower Eocene carbonate-rich sediments during the CIE recovery interval resulting from a post-PETM carbonate overshoot (Penman et al., 2016) and also contains an ~10-cm-thick silicified claystone within the CIE. The Paleocene-Eocene boundary at Site U1408, although condensed, features an ~20-cm-thick siliceous limestone capped by a centimeter-scale chert layer, bracketed by upper Paleocene and lower Eocene nanofossil chalk. The PETM at Site U1409 features a sequence (in decreasing depth and age) of siliceous limestone, claystone (the CIE interval), siliceous claystone (most of the CIE recovery), and an ~3 cm chert, with nanofossil chalk below and above the event. Shipboard X-ray diffraction analyses of the silicified portions of the Site U1409 Paleocene-Eocene boundary interval indicated the presence of cristobalite-tridymite (CT) as well as quartz, suggesting partial conversion of biogenic opal to chert (Norris et al., 2012). At Site U1409 the lowest appearance of siliceous limestone begins 12 cm below the CIE onset. However, as this sequence has undergone partial silica diagenesis, it is likely that any SiO<sub>2</sub> deposited as opal during the PETM would have vertically migrated on pore-water diffusional length scales during its dissolution and subsequent reprecipitation as CT and/or chert, such that some fraction of biogenic opal deposited during the CIE interval could easily have reprecipitated in the 12 cm underlying the CIE. Site U1407 consists of nanofossil chalk from both the late Paleocene and early Eocene, however no Paleocene-Eocene boundary was recovered due to a particularly well-lithified (presumably silicified due to increasing silicification of immediately over- and under-lying sediments) interval of ~20 m thickness.

The occurrence of silicified PETM sediments in all four sites, separated by hundreds of kilometers in distance and almost 2 km in water depth, demonstrates a regional unit of siliceous sediments in association with the PETM CIE ranging in thickness from centimeter scale

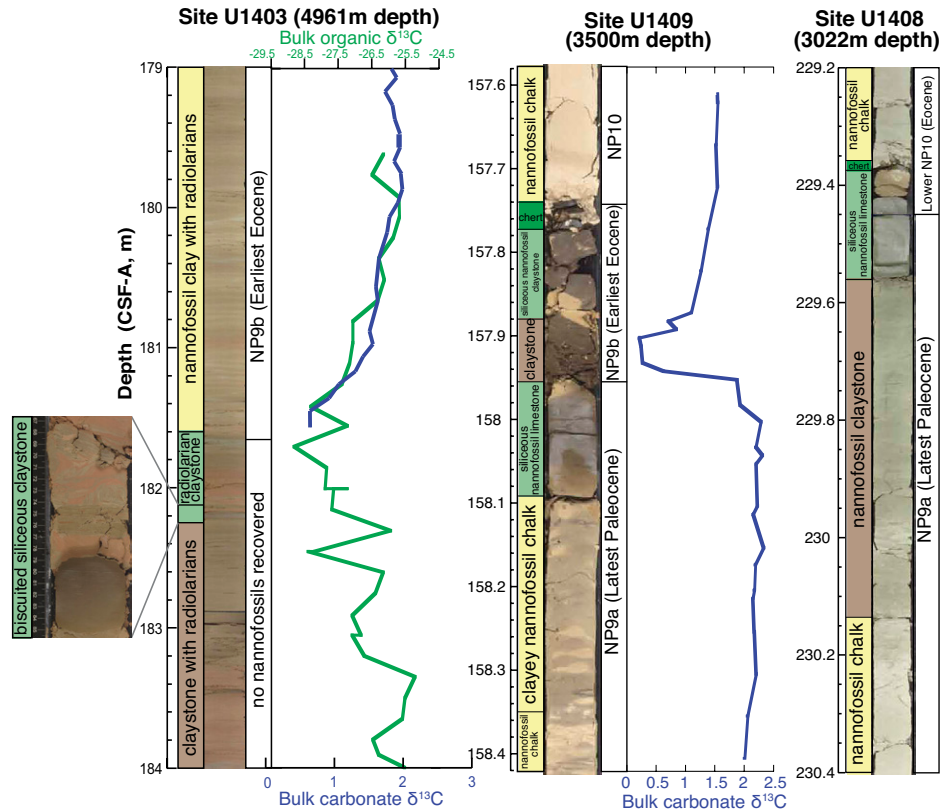


**Figure 3. New records of the Paleocene-Eocene Thermal Maximum (PETM) from the North Atlantic. Shown are core photographs (Integrated Ocean Drilling Program [IODP] Site U1403 is vertically compressed except for inset, other sites are to scale), lithologic description, nanofossil zones, and δ<sup>13</sup>C (IODP Sites U1403 and U1409 only). Lithology is color coded for major constituents: clays in brown, carbonates in yellow, and silicified sediments in green. For sediment classification methodology, see Norris et al. (2012). CSF-A depth scale is hole-specific meters below seafloor (previously mbsf).**

(IODP Site U1403) to at least tens of centimeters (Sites U1408 and U1409) and possibly up to several meters (Site U1407). The common occurrence of radiolarians in upper Paleocene sediments at all four sites is consistent with the derivation of these cherts through diagenetic alteration of biogenic silica. This spike in silica burial is rare amongst the dozens of deep-sea PETM sections described globally, and may represent the burial of anomalous Si weathered from continents during the PETM. Globally, few records show increased SiO<sub>2</sub> burial during the PETM, all from the Atlantic or Tethys: the Forada section in Italy demonstrates a spike in radiolarian abundance coincident with the CIE (Luciani et al., 2007), and in the Fur Formation (North Sea), an acme of the diatom *Fenestrella antiqua* serves as a practical regional marker for the base of the Eocene (Mittlehner, 1996). Conversely, a record from the Pacific shows little change in biogenic silica accumulation over the PETM (Murphy et al., 2006).

## DISCUSSION

In the context of the above calculations and modeling, it is expected that globally, sediments should show elevated SiO<sub>2</sub> burial during

the PETM. The question thus becomes: Why is elevated silica burial apparent only in the North Atlantic (and Tethys), and not globally?

Deep-ocean [H<sub>4</sub>SiO<sub>4</sub>] increases with ventilation age, as deep waters accumulate silica from the dissolution of sinking opal. Today, the formation of deep water in the North Atlantic and Southern Ocean and its aging into the North Pacific results in the lowest deep-water [H<sub>4</sub>SiO<sub>4</sub>] in the North Atlantic and the highest [H<sub>4</sub>SiO<sub>4</sub>] in the North Pacific (host to the oldest deep water). It has been suggested that during the PETM, a circulation change effectively reversed the deep-water ageing gradient relative to today (Bice and Marotzke, 2002; Zeebe and Zachos, 2007). Under such circulation, the Pacific would have contained H<sub>4</sub>SiO<sub>4</sub>-depleted, young deep water while the North Atlantic would have been host to the oldest, highest-[H<sub>4</sub>SiO<sub>4</sub>] deep waters. This could have focused elevated SiO<sub>2</sub> burial in the North Atlantic in two ways. First, upwelling H<sub>4</sub>SiO<sub>4</sub>-rich deep water might have fueled blooms of siliceous plankton which could have out-competed their calcareous counterparts because of higher [H<sub>4</sub>SiO<sub>4</sub>] and inhibition of calcification by ocean acidification during the PETM (Penman et al., 2014). Second, higher

[H<sub>4</sub>SiO<sub>4</sub>] would have slowed the dissolution of sinking opal in the water column and in sediments, ensuring that a greater fraction of opal precipitated at the surface reached sediments to be preserved and buried. By this mechanism, the elevated SiO<sub>2</sub> observed in the North Atlantic records is due both to enhanced weathering and the influence of circulation: globally integrated SiO<sub>2</sub> burial must have increased during the PETM as a result of elevated riverine Si input, while the apparent focusing of that burial in the North Atlantic may have been due to circulation change.

Muttoni and Kent (2007) listed 26 known chert deposits from ocean drilling sites that temporally overlap with the PETM (to which I add Sites U1403, U1408, and U1409), half of which are in the North Atlantic or Caribbean. While none of those cherts (with the exception of the records detailed here) have been associated with the PETM CIE (indeed, those cherts range from 1.2 to 28 m.y. in duration, too long to be attributable to the PETM specifically), the typically poor recovery and dating of silicified deep-sea sediments may have obscured enhanced silica burial during the PETM at some of those sites. It has been noted that the North Atlantic is host to abundant chert deposits laid down throughout the warm early to middle Eocene (ca. 46–54 Ma; Muttoni and Kent, 2007), most dramatically in the case of acoustic horizon A<sub>c</sub>, a chert horizon that covers most of the central North Atlantic (ca. 45–50 Ma; McGowran, 1989). It thus appears that the North Atlantic acted as a major silica sink during many of the greenhouse warming events and intervals of the early Cenozoic, of which the PETM is merely a prominent example.

#### ACKNOWLEDGEMENTS

I thank IODP Expedition 342 participants for the recovery and description of the new records, Ellen Thomas and Toby Tyrell for invaluable feedback, and David Archer and Kathleen Ritterbush for constructive reviews.

#### REFERENCES CITED

Berner, R.A., Lasaga, A.C., and Garrels, R.M., 1983, The carbonate-silicate geochemical cycle and its effects on atmospheric carbon dioxide over the past 100 million years: *American Journal of Science*, v. 283, p. 641–683, doi:10.2475/ajs.283.7.641.

Bice, K.L., and Marotzke, J., 2002, Could changing ocean circulation have destabilized methane hydrate at the Paleocene/Eocene boundary?: *Paleoceanography*, v. 17, p. 8–1–8–12, doi:10.1029/2001PA000678.

Bowen, G.J., and Zachos, J.C., 2010, Rapid carbon sequestration at the termination of the Palaeocene-Eocene Thermal Maximum: *Nature Geoscience*, v. 3, p. 866–869, doi:10.1038/ngeo1014.

Cui, Y., Kump, L.R., Ridgwell, A.J., Charles, A.J., Junium, C.K., Diefendorf, A.F., Freeman, K.H., Urban, N.M., and Harding, I.C., 2011, Slow release of fossil carbon during the Palaeocene-Eocene

Thermal Maximum: *Nature Geoscience*, v. 4, p. 481–485, doi:10.1038/ngeo1179.

Dickens, G.R., Castillo, M.M., and Walker, J.C.G., 1997, A blast of gas in the latest Paleocene: Simulating first-order effects of massive dissociation of oceanic methane hydrate: *Geology*, v. 25, p. 259–262, doi:10.1130/0091-7613(1997)025<0259:ABOGIT>2.3.CO;2.

Dunkley-Jones, T., Lunt, D.J., Schmidt, D.N., Ridgwell, A., Sluijs, A., Valdes, P.J., and Maslin, M., 2013, Climate model and proxy data constraints on ocean warming across the Paleocene-Eocene Thermal Maximum: *Earth-Science Reviews*, v. 125, p. 123–145, doi:10.1016/j.earscirev.2013.07.004.

Gaillardet, J., Dupré, B., Louvat, P., and Allègre, C.J., 1999, Global silicate weathering and CO<sub>2</sub> consumption rates deduced from the chemistry of large rivers: *Chemical Geology*, v. 159, p. 3–30, doi:10.1016/S0009-2541(99)00031-5.

Garrels, R.M., and Berner, R.A., 1983, The global carbonate-silicate sedimentary system: Some feedback relations, in Westbroek, P., and de Jong, E.W., eds., *Biominalization and Biological Metal Accumulation: Biological and Geological Perspectives*: Dordrecht, Netherlands, Springer, p. 73–87, doi:10.1007/978-94-009-7944-4\_6.

Harper, H.E., and Knoll, A.H., 1975, Silica, diatoms, and Cenozoic radiolarian evolution: *Geology*, v. 3, p. 175–177, doi:10.1130/0091-7613(1975)3<175:SDACRE>2.0.CO;2.

Kelly, D.C., Nielsen, T.M.J., McCarren, H.K., Zachos, J.C., and Röhl, U., 2010, Spatiotemporal patterns of carbonate sedimentation in the South Atlantic: Implications for carbon cycling during the Paleocene-Eocene thermal maximum: *Paleoceanography*, *Paleoclimatology*, *Paleoecology*, v. 29, p. 30–40, doi:10.1016/j.palaeo.2010.04.027.

Kennett, J.P., and Stott, L.D., 1991, Abrupt deep-sea warming, paleoceanographic changes and benthic extinctions at the end of the Paleocene: *Nature*, v. 353, p. 225–229, doi:10.1038/353225a0.

Luciani, V., Giusberti, L., Agnini, C., Backman, J., Fornaciari, E., and Rio, D., 2007, The Paleocene-Eocene Thermal Maximum as recorded by Tethyan planktonic foraminifera in the Forada section (northern Italy): *Marine Micropaleontology*, v. 64, p. 189–214, doi:10.1016/j.marmicro.2007.05.001.

McGowran, B., 1989, Silica burp in the Eocene ocean: *Geology*, v. 17, p. 857–860, doi:10.1130/0091-7613(1989)017<0857:SBITEO>2.3.CO;2.

McInerney, F.A., and Wing, S., 2011, The Paleocene-Eocene Thermal Maximum: A perturbation of carbon cycle, climate, and biosphere with implications for the future: *Annual Review of Earth and Planetary Sciences*, v. 39, p. 489–516, doi:10.1146/annurev-earth-040610-133431.

Mitlehner, A.G., 1996, Palaeoenvironments in the North Sea Basin around the Paleocene-Eocene boundary: Evidence from diatoms and other siliceous microfossils, in Knox, R.W.O'B., et al., eds., *Correlation of the Early Paleogene in Northwest Europe*: Geological Society of London Special Publication 101, p. 255–273, doi:10.1144/GSL.SP.1996.101.01.15.

Murphy, B., Lyle, M., and Lyle, A.O., 2006, Biogenic burial across the Paleocene/Eocene boundary: Ocean Drilling Program Leg 199 Site 1221, in Wilson, P.A., et al., eds., *Proceedings of the Ocean Drilling Program, Scientific Results, Volume 199*: College Station, Texas, Ocean Drilling Program, doi:10.2973/odp.proc.sr.199.215.2006.

Murphy, B.H., Farley, K.A., and Zachos, J.C., 2010, An extraterrestrial <sup>3</sup>He-based timescale for the

Paleocene-Eocene thermal maximum (PETM) from Walvis Ridge, IODP Site 1266: *Geochimica et Cosmochimica Acta*, v. 74, p. 5098–5108, doi:10.1016/j.gca.2010.03.039.

Muttoni, G., and Kent, D.V., 2007, Widespread formation of cherts during the early Eocene climate optimum: *Paleoceanography*, *Paleoclimatology*, *Paleoecology*, v. 25, p. 348–362, doi:10.1016/j.palaeo.2007.06.008.

Norris, R.D., Wilson, P.A., Blum, P., and the Expedition 342 Scientists, 2014, *Proceedings of the Integrated Ocean Drilling Program, Preliminary Reports*, v. 342: College Station, Texas, Integrated Ocean Drilling Program, 63 p., doi:10.2204/iodp.proc.342.2014.

Penman, D.E., Hönisch, B., Zeebe, R.E., Thomas, E., and Zachos, J.C., 2014, Rapid and sustained surface ocean acidification during the Paleocene-Eocene Thermal Maximum: *Paleoceanography*, v. 29, p. 357–369, doi:10.1002/2014PA002621.

Penman, D.E., et al., 2016, An abyssal carbonate compensation depth overshoot in the aftermath of the Palaeocene-Eocene Thermal Maximum: *Nature Geoscience*, v. 9, p. 575–580, doi:10.1038/NNGEO2757.

Racki, G., and Cordey, F., 2000, Radiolarian paleoecology and radiolarites: Is the present the key to the past?: *Earth-Science Reviews*, v. 52, p. 83–120, doi:10.1016/S0012-8252(00)00024-6.

Ravizza, G., Norris, R.N., Blusztajn, J., and Aubry, M.P., 2001, An osmium isotope excursion associated with the late Paleocene thermal maximum: Evidence of intensified chemical weathering: *Paleoceanography*, v. 16, p. 155–163, doi:10.1029/2000PA000541.

Ritterbush, K.A., Rosas, S., Corsetti, F.A., Bottjer, D.J., and West, A.J., 2015, Andean sponges reveal long-term benthic ecosystem shifts following the end-Triassic mass extinction: *Paleoceanography*, *Paleoclimatology*, *Paleoecology*, v. 420, p. 193–209, doi:10.1016/j.palaeo.2014.12.002.

Torfstein, A., Winckler, G., and Tripathi, A., 2010, Productivity feedback did not terminate the Paleocene-Eocene Thermal Maximum (PETM): *Climate of the Past*, v. 6, p. 265–272, doi:10.5194/cp-6-265-2010.

Treguer, P., Nelson, D.M., Van Bennekom, A.J., and DeMaster, D.J., 1995, The silica balance in the world ocean: A reestimate: *Science*, v. 268, p. 375–379, doi:10.1126/science.268.5209.375.

Yool, A., and Tyrell, T., 2003, Role of diatoms in regulating the ocean's silicon cycle: *Global Biogeochemical Cycles*, v. 17, 1103, doi:10.1029/2002GB002018.

Yool, A., and Tyrell, T., 2005, Implications for the history of Cenozoic opal deposition from a quantitative model: *Paleoceanography*, *Paleoclimatology*, *Paleoecology*, v. 218, p. 239–255, doi:10.1016/j.palaeo.2004.12.017.

Zeebe, R.E., and Zachos, J.C., 2007, Reversed deep-sea carbonate ion basin gradient during Paleocene-Eocene thermal maximum: *Paleoceanography*, v. 22, PA3201, doi:10.1029/2006PA001395.

Zeebe, R.E., Zachos, J.C., and Dickens, G.R., 2009, Carbon dioxide forcing alone insufficient to explain Palaeocene-Eocene Thermal Maximum warming: *Nature Geoscience*, v. 2, p. 576–580, doi:10.1038/ngeo578.

Manuscript received 19 January 2016

Revised manuscript received 22 June 2016

Manuscript accepted 23 June 2016

Printed in USA